Metabolic signatures of rhizobacteria-induced plant growth promotion

Plant, Cell & Environment

Jeon, Je-Seung; Rybka, D.J.; Carreno Quintero, N.; Vos, C.H.; Raaijmakers, J.M. et al

https://doi.org/10.1111/pce.14385

This publication is made publicly available in the institutional repository of Wageningen University and Research, under the terms of article 25fa of the Dutch Copyright Act, also known as the Amendment Taverne. This has been done with explicit consent by the author.

Article 25fa states that the author of a short scientific work funded either wholly or partially by Dutch public funds is entitled to make that work publicly available for no consideration following a reasonable period of time after the work was first published, provided that clear reference is made to the source of the first publication of the work.

This publication is distributed under The Association of Universities in the Netherlands (VSNU) 'Article 25fa implementation' project. In this project research outputs of researchers employed by Dutch Universities that comply with the legal requirements of Article 25fa of the Dutch Copyright Act are distributed online and free of cost or other barriers in institutional repositories. Research outputs are distributed six months after their first online publication in the original published version and with proper attribution to the source of the original publication.

You are permitted to download and use the publication for personal purposes. All rights remain with the author(s) and / or copyright owner(s) of this work. Any use of the publication or parts of it other than authorised under article 25fa of the Dutch Copyright act is prohibited. Wageningen University & Research and the author(s) of this publication shall not be held responsible or liable for any damages resulting from your (re)use of this publication.

For questions regarding the public availability of this publication please contact openscience.library@wur.nl

Received: 12 July 2019 | Revised: 21 May 2022 | Accepted: 22 June 2022

DOI: 10.1111/pce.14385

ORIGINAL ARTICLE

Plant, Cell & Environment PC&E WILEY

Metabolic signatures of rhizobacteria-induced plant growth promotion

Je-Seung Jeon[1,2] | Dominika Rybka[1] | Natalia Carreno-Quintero[1,3] | Ric De Vos[4] | Jos M. Raaijmakers[1,2] | Desalegn W. Etalo[1,5]

[1]Department of Microbial Ecology, Netherlands Institute of Ecology NIOO-KNAW, Wageningen, The Netherlands

[2]Institute of Biology, Leiden University, Leiden, The Netherlands

[3]KeyGene, Wageningen, The Netherlands

[4]Wageningen Plant Research, Bioscience, Wageningen, The Netherlands

[5]Laboratory of Phytopathology, Wageningen University and Research, Wageningen, The Netherlands

Correspondence
Jos M. Raaijmakers and Desalegn W. Etalo, Department of Microbial Ecology, Netherlands Institute of Ecology NIOO-KNAW, Wageningen, 6708 PB, The Netherlands.
Email: j.raaijmakers@nioo.knaw.nl and D.Etalo@nioo.knaw.nl

Funding information
BEBasic, Grant/Award Number: 7.3.4; Korean government scholarship program of the National Institute for International Education (NIIED)

Abstract

Various root-colonizing bacterial species can promote plant growth and trigger systemic resistance against aboveground leaf pathogens and herbivore insects. To date, the underlying metabolic signatures of these rhizobacteria-induced plant phenotypes are poorly understood. To identify core metabolic pathways that are targeted by growth-promoting rhizobacteria, we used combinations of three plant species and three rhizobacterial species and interrogated plant shoot chemistry by untargeted metabolomics. A substantial part (50%–64%) of the metabolites detected in plant shoot tissue was differentially affected by the rhizobacteria. Among others, the phenylpropanoid pathway was targeted by the rhizobacteria in each of the three plant species. Differential regulation of the various branches of the phenylpropanoid pathways showed an association with either plant growth promotion or growth reduction. Overall, suppression of flavonoid biosynthesis was associated with growth promotion, while growth reduction showed elevated levels of flavonoids. Subsequent assays with 12 Arabidopsis flavonoid biosynthetic mutants revealed that the proanthocyanidin branch plays an essential role in rhizobacteria-mediated growth promotion. Our study also showed that a number of pharmaceutically and nutritionally relevant metabolites in the plant shoot were significantly increased by rhizobacterial treatment, providing new avenues to use rhizobacteria to tilt plant metabolism towards the biosynthesis of valuable natural plant products.

KEYWORDS

bacteria-plant interactions, beneficial rhizobacteria, flavonoids, high-value natural products, metabolic alterations, phenylpropanoids, plant metabolomics

1 | INTRODUCTION

The rhizosphere, the narrow zone surrounding and influenced by plant roots, harbours a plethora of microorganisms that can have deleterious or beneficial effects on plant growth and health (Mendes et al., 2011; Raaijmakers et al., 2009). Among the best-studied beneficial rhizosphere microbes are the plant growth-promoting rhizobacteria (PGPR). Their beneficial association is thought to be ancient and presumably has been shaped by co-evolutionary processes in the long-term interactions with their host plants (Lambers et al., 2009). PGPR can enhance plant growth through direct and indirect mechanisms (Lugtenberg & Kamilova, 2009). The direct mechanisms involve the facilitation of nutrient acquisition and modulation of phytohormones, whereas indirect effects involve suppression of biotic stress factors through parasitism, antibiosis, competition and the induction of systemic resistance (De Vleesschauwer & Höfte 2009; Pineda et al., 2010; Stringlis, Zhang, et al., 2018; Van der Ent et al., 2009; van Loon et al., 1998).

PGPR can also have profound effects on the physiology and metabolism of their host plants, not only by enhancing the production of known secondary metabolites but also by inducing the biosynthesis of yet-unknown compounds (Etalo et al., 2018; van de Mortel et al., 2012). The plant secondary metabolites affected by PGPR reported to date include, among others, polyphenols, flavonoids and glucosinolates but also primary metabolites such as carbohydrates and amino acids (Etalo et al., 2018). So far, only a few studies have provided mechanistic insights into the association between rhizobacteria-induced biochemical changes and plant growth and defense (Etalo et al., 2018; Hu et al., 2018; van de Mortel et al., 2012; Stringlis, Yu, et al., 2018; Walker et al., 2011; Weston et al., 2012).

PGPR can prime plant defense against pathogens and insect herbivores and at the same time promote plant growth. This is in contrast to the widely accepted trade-off between plant defense and plant fitness in general and plant growth in particular. Understanding the underlying plant metabolic networks and unravelling their interactions is essential to understand and optimize rhizobacteria-mediated growth promotion and induced systemic resistance (ISR). Although some reports indicated that rhizobacteria change specific classes of plant metabolites (Chamam et al., 2013; Mishra et al., 2006; Walker et al., 2011), their overarching effects on the global metabolome of plants and in particular on core metabolite pathways co-occurring with growth promotion across plant species are not well understood. In this context, PGPR-mediated re-routing of the plant's metabolism could give insight into the metabolic interplay between plant defense and growth. Furthermore, it is highly instrumental to understand the organization of metabolite routes and how rhizobacteria tilt a particular pathway towards a desired plant phenotype or the enhanced production of high-value plant compounds (HVPC) (Etalo et al., 2018).

Here, we studied the impact of three strains of different rhizobacterial genera on the phenotype and shoot metabolome of three plant species: *Arabidopsis thaliana* (model plant), *Brassica olearacea* var. italica (crop) and *Artemisia annua* (medicinal plant). The rhizobacterial strains *Paraburkholderia graminis* PHS1 (*Pbg*) (Carrión et al., 2018) and *Microbacterium* EC8 (MB) (Cordovez et al., 2018) were originally isolated from the rhizosphere of sugar beet (*Beta vulgaris*). *Pseudomonas fluorescens* SS101 (*Pf* SS101) was isolated from the wheat rhizosphere (De Souza et al., 2003). These rhizobacteria showed growth-promoting and pathogen-protective effects in different plant species (Carrión et al., 2018; Cheng et al., 2017; Cordovez et al., 2018; van de Mortel et al., 2012; Jeon et al., 2021; Tran et al., 2007). Here, our primary goal was to identify core metabolic pathways that are targeted by rhizobacteria in different plant species and to investigate the metabolomic changes induced in rhizobacteria-plant interactions that lead to either plant growth promotion (effective partnership) or to growth reduction and/or stress-related phenotypes (ineffective partnership). Integration of in vitro bioassays, untargeted metabolomics and screening of pathways-specific mutants showed that inoculation of the plant root system with each of the three rhizobacterial genera induced substantial changes in the shoot metabolome in a species-specific manner. The results pointed to the phenylpropanoid pathway as a central plant metabolome response associated with effective or ineffective partnerships. Subsequent analysis of 12 Arabidopsis *transparent testa* (*tt*) mutants defective in different branches of the flavonoid pathway, revealed that the proanthocyanidin (PA) branch is key in rhizobacteria-mediated plant growth promotion.

2 | MATERIALS AND METHODS

2.1 | Plant material

Seeds of *A. thaliana* flavonoid *transparent testa* (*tt*) mutants were obtained from Nottingham Arabidopsis Stock centre. *A. annua* (Artemisia F1 seeds, Hyb8001r) was provided by the Center for Novel Agriculture Products, Department of Biology, University of York, England. Seeds of *B. olearacea* var. italica, cultivar Coronado were provided by Bejo seeds, Warmenhuizen, the Netherlands.

2.2 | Seed surface sterilization

Seeds of Arabidopsis and Artemisia were surface sterilized as previously described by (van de Mortel et al., 2012). Briefly, the seeds were placed in opened Eppendorf tubes inside a desiccator with two 100-ml beakers each containing 50 ml sodium hypochlorite (12% v/v). To each of the beakers, 1.5 ml concentrated HCl was added and the seeds were exposed for 3 h to the chlorine gas generated inside the desiccator. Seeds of *B. olearacea* var. italica, cultivar Coronado were surface-sterilized for 30 min in 1% (v/v) sodium hypochlorite supplemented with 0.1% (v/v) Tween 20 and then washed three times with ample sterile distilled water.

2.3 | Bacterial strains and culture conditions

P. fluorescens SS101 (*Pf* SS101) was cultured in King's medium B (KB), while *Microbacterium* EC8 (MB) was cultured in Tryptone Soy broth (TSB) medium and *P. graminis* PHS1 (*Pbg*) in Luria Bertani (LB) medium (Lennox, Carl Roth) at 25°C for 16 h. Bacterial cells were collected by centrifugation, washed three times with 10 mM $MgSO_4$ and resuspended in 10 mM $MgSO_4$ to a final density of ~10^9 cells/ml ($OD_{600} = 1.0$).

2.4 | Plant phenotyping

After surface sterilization, seeds of Arabidopsis and Broccoli were pre-germinated on sterile wet filter paper in plastic petri dishes and placed at 4°C in the dark for 4 and 2 days, respectively. After the emergence of the radicle, seeds were sown on half-strength

Murashige and Skoog (MS) medium containing 2.5% (w/v) sucrose and plant agar 1,2%. The plates were then transferred to a climate chamber at 21°C/21°C day/night; 180 µmol light $m^{-2}s^{-1}$, 16 h light/8 h dark cycle and 70% relative humidity. The root tips of the seedlings were inoculated with 2 µl of washed bacterial cell suspension ($OD_{600} = 1.0$) 7 days postplanting for *A. thaliana* and *A. annua* and after 3 days for *B. oleracea*; the plants were grown in the same growth chamber until harvest. To assess the temporal changes in plant growth of the different plant species-rhizobacteria combinations, the shoot fresh biomass was determined every two days until 11 days postinoculation (dpi) for Arabidopsis and Broccoli and until 14 dpi for Artemisia. For each plant species, four independent biological replicates were considered with 10 seedlings of Arabidopsis, 8 of Artemisia and 5 of Broccoli per biological replicate. Before root dry mass measurements, roots were carefully detached from the MS-agar and washed with sterile distilled water to remove agar. Thereafter, root dry biomass was determined (Ostonen et al., 2007).

2.5 | Rhizobacteria colonization

Bacterial root colonization was determined at 11 dpi for Arabidopsis and Broccoli and at 14 dpi for Artemisia. Roots were collected in sterile glassware and their fresh weight was determined. Root samples were vortexed for 60 s in 10 mM $MgSO_4$, sonicated for 60 s and vortexed once more for 15 s. After serial dilution, 50 µl of the suspensions were plated onto PSA (*Pf* SS101 and *Pbg*) and TSA (MB) containing 100 µg ml^{-1} delvocid (DSM), an antifungal agent. After 3 days of incubation at 25°C, the number of colonies were counted for each of the replicates. Bacterial colonization was expressed as colony-forming units (CFU) per gram of root fresh weight.

2.6 | Plant metabolite analysis

2.6.1 | Sample collection and extraction

Shoots were harvested at 11 dpi for Arabidopsis ($N = 10$) and Broccoli ($N = 5$) seedlings and at 14 dpi for Artemisia ($N = 8$). For each plant species × rhizobacteria combination, four biological replicates comprising the aforementioned number of plants were used. Briefly, shoots were snap-frozen in liquid nitrogen and ground to a fine powder under continuous cooling and kept at −80°C until further use. For extraction of semipolar metabolites, 300 µl of 99.89% methanol containing 0.13% (v/v) formic acid (FA) was added to 100 mg powdered plant material in 2 ml round-bottom Eppendorf tubes and sonicated for 15 min followed by centrifugation for 15 min at 20 000*g*. The supernatants were transferred to a 96-well plate (AcroPrepTM, 350 µl, 0.45 µm, PALL) and vacuum filtrated into a 96-deep-well autosampler plate (Waters) using a Genesis Workstation (Tecan Systems).

2.6.2 | Metabolite analysis

An UltiMate 3000 U-HPLC system (Dionex) was used to create a 45 min linear gradient of 5%–35% (v/v) acetonitrile in 0.1% (v/v) FA in water at a flow rate of 0.19 ml min^{-1}. Five microlitres of each extract was injected and compounds were separated on a Luna C18 column (2.0 × 150 mm, 3 µm; Phenomenex) maintained at 40°C (De Vos et al., 2007). The detection of compounds eluting from the column was performed with a Q-Exactive Plus Orbitrap FTMS mass spectrometer (Thermo Scientific). Full scan MS data were generated with electrospray in switching positive/negative ionization mode at a mass resolution of 35 000 (FWHM at m/z 200) in a range of m/z 95–1350. Subsequent MS/MS experiments for the identification of selected metabolites were performed with separate positive or negative electrospray ionization at a normalized collision energy of 27 and a mass resolution of 17 500. The ionization voltage was optimized at 3.5 kV for positive mode and 2.5 kV for negative mode; the capillary temperature was set at 250°C; the auxiliary gas heater temperature was set to 220°C; sheath gas, auxiliary gas and the sweep gas flow were optimized at 36, 10 and 1 arbitrary units, respectively. Automatic gain control was set at 3 e^6 and the injection time at 100 ms. External mass calibration with FA clusters was performed in both positive and negative ionization modes before each sample series.

2.6.3 | Liquid chromatography-mass spectrometry (LC-MS) data processing and analysis

Mass peak picking and alignment were performed using Metalign software (Lommen 2009). Mass features in the resulting peak list were considered as a real signal if they were detected with an intensity of more than three times the noise value and in three out of the four biological replicates of at least one treatment. Mass features originating from the same metabolites were subsequently reconstituted based on their similar retention window and their intensity correlation across all measured samples, using MSClust software (Tikunov et al., 2012). This resulted in the relative intensity of 725 putative metabolites in Arabidopsis, 868 in Artemisia and 1908 in broccoli detected in positive and negative ionization mode, in which the metabolite abundance was represented by the Measured Ion Count (MIC), that is, the sum of the corrected intensity values of all mass features ions within the corresponding cluster. Log transformation and scaling of the data were performed in GeneMaths XT 1.6 (www.applied-maths.com). Transformed and scaled values were used for the analysis of variance (ANOVA) with correction for multiple testing (Benjamini and Hochberg) to pinpoint compounds that were significantly different between the treatments ($p < 0.05$, fold change >2). The differentially accumulated metabolites were used for principal component analysis (PCA) and hierarchical cluster analysis (HCA) to investigate and visualize metabolite clusters that were significantly altered in a rhizobacteria-plant-specific manner (Figure 2). The HCA was performed using Pearson's correlation and

Unweighted Pair Group Method with Arithmetic Mean (UPGMA) method.

Annotation of differential metabolites was performed after manually identifying the putative molecular ions within the clustered masses. In-house databases were used to annotate metabolites detected in Arabidopsis and Broccoli by considering the observed accurate masses and retention times of the molecular ions. If selected compounds were not yet present in this experimentally obtained database, detected masses were matched with compound libraries, including Metabolomics Japan (www.metabolomics.jp), the Dictionary of Natural Products (www.dnp.chemnetbase.com), KNApSAcK (www.knapsackfamily.com) and Metlin (www.metlin.scripps.edu) using a maximum mass deviation of 5 ppm. To annotate metabolites detected in Artemisia, we used the online Magma (Ridder et al., 2013) in combination with the abovementioned publicly available databases.

2.7 | Statistical analysis of plant phenotypic data

The relative changes in shoot biomass, root biomass in the combinations of the three plants and three rhizobacterial strains were analyzed with R Studio (Version 3.5.2). First, the normality and homogeneity of variance of the data was assessed and when the two assumptions were not met, the data was subjected to Box-Cox transformation using the package MASS. Differences were tested by two-way ANOVA. A Tukey-honestly significant difference test was used to separate group mean values when the ANOVA was significant at $p < 0.05$. The ANOVA table is shown in Supporting Information: Table S1. Differences between rhizobacterial treatments and nontreated control on raw phenotype parameters were compared by Student's t-test.

3 | RESULTS

3.1 | Plant growth promotion is bacteria and plant species-specific

To assess the changes in the growth of Arabidopsis (model plant), Artemisia (medicinal plant) and Broccoli (crop) induced by strains of three specific rhizobacterial genera (Figure 1a), we expressed fresh root and shoot biomass as a percentage relative to the nontreated control plants. Two-way ANOVA showed that the impact of the three rhizobacterial strains on plant growth was dependent on the interacting partners (Supporting Information: Table S1). In the following sections, we refer to these interactions as ‘effective partnerships’ when the rhizobacterial strain promotes growth

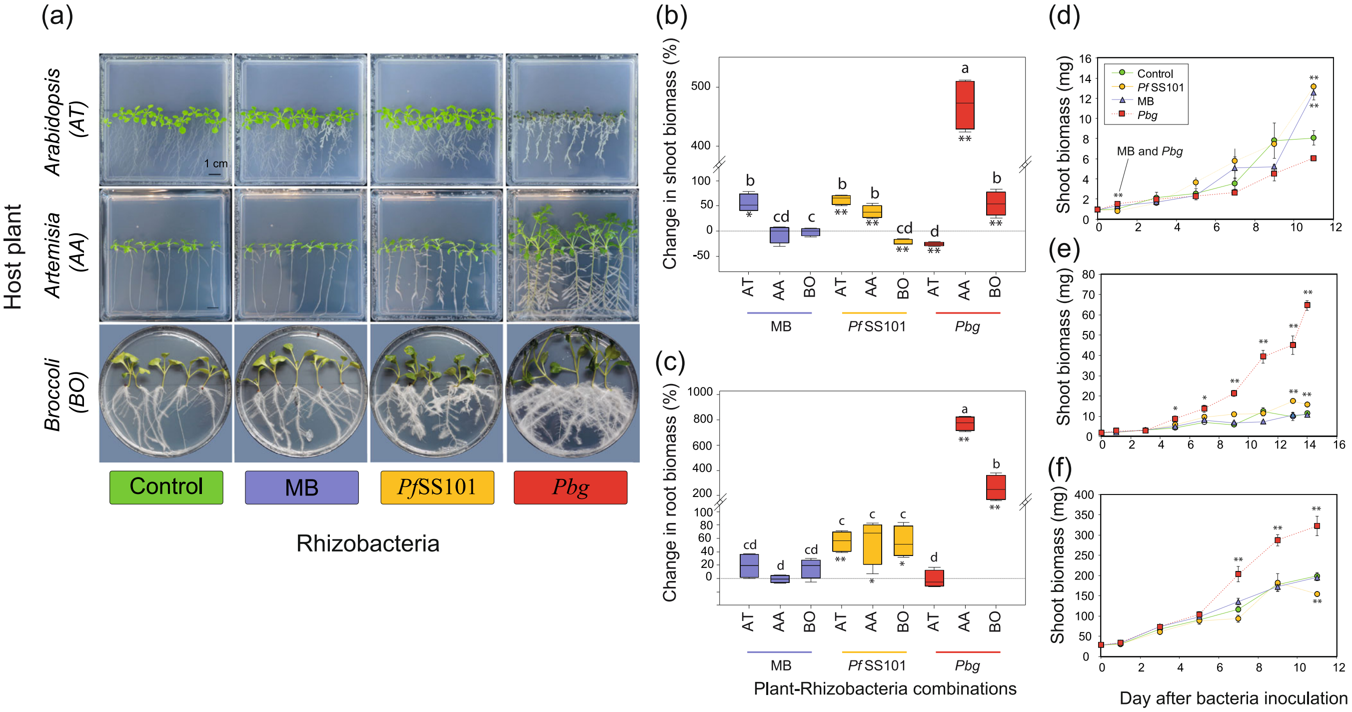

FIGURE 1 Phenotypic changes in response to rhizobacteria inoculation. Photographs of Murashige and Skoog agar plates with Arabidopsis, Artemisia and Broccoli seedlings at 11, 14 and 11 dpi, respectively (a). Percent change in shoot fresh biomass (b). Percent change in root fresh biomass (c). Temporal growth dynamics of Arabidopsis (d), Artemisia (e) and Broccoli (f) after inoculation with three distinct rhizobacterial strains; *Pseudomonas fluorescens* SS101(PfSS101), Microbacterium sp EC8 (MB) and *Paraburkholderia graminis* mHS1(Pbg). Asterisks denote statistical differences (two-tailed Student's t-test): * $p < 0.05$; ** $p < 0.01$. Data are mean ± standard error (SE); ($n = 4$ biological replicates). For each biological replicate 10 Arabidopsis, 8 Artemisia and 5 Broccoli seedlings were used. Means sharing the same letter are not significantly different based on two-way analysis of variance (Tukey, $p < 0.05$). [Color figure can be viewed at wileyonlinelibrary.com]

whereas 'ineffective partnerships' result in no growth promotion or reduced growth including stress-related phenotype (Figure 1b,c).

3.1.1 | Effective partnerships

Root tip inoculation with *P. fluorescens* strain *Pf*SS101 resulted in a significant increase in shoot biomass in both Arabidopsis and Artemisia (63.1% ± 4.7 and 38.7% ± 6.3, respectively) (Figure 1b). Similarly, root tip inoculation with *P. graminis* strain PHS1 (*Pbg*) resulted in significant increases in shoot biomass of both Artemisia and Broccoli (470.4% ± 21.3 and 54.1% ± 11.9, respectively). With a biomass increase of almost fivefold relative to the untreated control plants, *Pbg*-Artemisia was considered as the most effective partnership. Likewise, the effect of the rhizobacterial strains on root biomass and architecture was highly species-specific (Figure 1a,c and Supporting Information: Figure S1). *Pbg* resulted in significant increases in root biomass in both Artemisia and Broccoli (773.9% [±28.2] and 258.8% [±50.1], respectively) (Figure 1c). Inoculation of MB induced a significant increase in shoot biomass only in Arabidopsis. The best-performing partnerships were characterized by an early and sustained growth promotion (Figure 1d–f). For example, *Pbg*-Artemisia showed a significant increase in shoot fresh biomass as early as 5 dpi, while growth promotion in the combination of *Pf* SS101-Artemisia was only apparent after 13 dpi (Figure 1e). *Pbg*-Broccoli showed a significant and sustained plant growth promotion at 7 dpi compared to the control plants (Figure 1f). In Arabidopsis, only *Pf*SS101 and MB induced a significant increase in shoot biomass (Figure 1d).

3.1.2 | Ineffective partnerships

Root tip inoculation of *Pf*SS101 resulted in a significant reduction (−22% ± 2.6) of shoot biomass in Broccoli. Similarly, inoculation of Arabidopsis with *Pbg* significantly reduced shoot biomass (−24.9% ± 1.8). Root tip inoculation of both Artemisia and Broccoli with MB had no significant impact on both shoot and root biomass (Figure 1b,c).

3.2 | Relationship between growth promotion and root colonization

In the assays described above, root colonization was assessed when plants were 11 days old. For Arabidopsis, Broccoli and Artemisia, *Pf* SS101 established population densities ranging from $1.5 \pm 0.1 \times 10^5$ to $9.4 \pm 0.7 \times 10^7$ CFU mg^{-1} root fresh weight. In contrast, MB colonization of roots varied greatly between different plant species: MB established population densities on Arabidopsis roots of $7.5 \pm 0.5 \times 10^6$ CFU mg^{-1}, whereas MB densities on Artemisia roots were below the detection limit. *Pbg* colonized roots of all three plant species at relatively high densities ranging from $8.1 \pm 0.3 \times 10^7$ to $1.0 \pm 0.1 \times 10^9$ CFU mg^{-1} (Supporting Information: Table S2). To determine correlations, if any, between the rhizosphere population densities and specific plant phenotypes (i.e., biomass), we plotted the rhizobacterial densities against various plant parameters (Supporting Information: Figure S2). Colonization of the root at higher density showed a positive, negative or no association with shoot and root biomass and depended on the host-rhizobacterium combination. For example, *Pbg* reached higher population densities than *Pf* SS101 and MB on the root of Arabidopsis and Artemisia. In Arabidopsis, high population densities of *Pbg* were associated with a reduction in shoot biomass while in Artemisia it resulted in significant enhancement of shoot biomass. In Broccoli, all three rhizobacterial strains showed a similar level of root colonization, yet the plant phenotype varied greatly: *Pbg* induced a significant increase in shoot biomass while *Pf* SS101 resulted in a significant reduction in shoot biomass and MB showed no significant effect on shoot biomass. Hence, there was no clear overall correlation between rhizosphere population densities of the introduced rhizobacterial strains and shoot/root biomass (Supporting Information: Figures S2a,b).

3.3 | Global and specific rhizobacteria-induced changes in the plant shoot metabolome

Liquid chromatography-mass spectrometry(LC-MS)-based nontargeted metabolite profiling was used to investigate the global and specific effects of each of the three rhizobacterial strains on the occurrence and relative abundance of semipolar secondary metabolites in shoots of Arabidopsis, Artemisia and Broccoli. Emphasis was given to metabolic alterations that differentiate effective from ineffective plant-rhizobacteria partnerships. An overview of metabolites that were significantly increased or reduced revealed that root inoculation with *Pbg* exerted the largest alteration of the shoot metabolomes of Artemisia and Arabidopsis, combinations that represent the most effective and ineffective partnerships, respectively (Supporting Information: Figure S3 and Table S3). Furthermore, most of the differential metabolites were unique for plants inoculated with *Pbg*, that is, they were below the detection limit in untreated control plants. In Broccoli, the ineffective partnership with *Pf*SS101 accounted for the largest share of the 'upregulated' metabolites, whereas its effective partnership with *Pbg* accounted for the largest share of 'downregulated' metabolites (Supporting Information: Figure S3 and Table S3).

3.3.1 | Arabidopsis

Inoculation of Arabidopsis roots with each of the three rhizobacteria resulted in significant changes in the shoot metabolome. From the 725 detected metabolites, 465 (64%) were significantly different between at least two treatments. In the PCA, the first three principal components explained 89% of the total variance (Figure 2a1). The first principal component (PC1), representing 56% of the total variance, was associated with metabolites that were highly induced (Figure 2a2 clusters **5**; 291 metabolites and **6**; 10 metabolites) or reduced in the ineffective partnership between *Pbg* and Arabidopsis (clusters **3**; 82 metabolites and **4**; 33 metabolites). *Pbg*-induced metabolites in cluster **5** primarily encompassed flavonoids including anthocyanins (cyanidin rutinoside, delphinidin rutinoside), tryptophan and its derivatives such as IAA, defense or stress-associated metabolites such as salicylic acid, dihydroxybenzoic acid glucosides, scopolin and camalexin. The second principal component (PC2) explained 21% of the total variance and corresponded to metabolites that were increased (Figures 2a1,a2 clusters **2**; 18 metabolites and **6**; 9 metabolites) or decreased (cluster **7**; 10 metabolites) in the effective partnership of Arabidopsis with *Pf* SS101 and MB. Among the identified metabolites, the long-chain aliphatic glucosinolate glucohirsutin (8-(methylsulfinyl)octyl glucosinolate) was significantly increased in Arabidopsis shoot after inoculation with *Pf* SS101 or MB. From the same group of glucosinolates, 8-(methylthio) octyl glucosinolate was significantly increased after inoculation with *Pf* SS101 (Supporting Information: Table S4). The third principal component (PC3) explained 12% of the total variation and was represented by metabolites that accumulated only after inoculation with either *Pf* SS101 or MB (Figure 2a1,a2 cluster **1**; 8 metabolites and cluster **9**; 7 metabolites, respectively). A fatty acyl glycoside demonstrated *Pf* SS101-specific accumulation while fumaric acid displayed MB-specific increases.

3.3.2 | Artemisia

From the 868 metabolites that were detected in the Artemisia shoot samples, 451 (52%) metabolites were significantly different between at least two rhizobacteria treatments. In the PCA, the first two PCs explained 80% of the total variance (Figure 2b1). The first principal component explained more than 64% of the total variance and corresponds to metabolites that were either reduced or accumulated during the most effective partnership of the host with *Pbg* (Figure 2b1,b2 cluster **1** [reduced metabolites] and cluster **2** [induced metabolites]). Flavanones, flavonol glycosides, coumarins, benzoic acid derivatives, acylated polyamine, catechols, fatty acyl glycosides of mono- and disaccharides, dipeptide and terpene glycosides showed significant reductions upon *Pbg* inoculation. Various other metabolites belonging to the compound classes hydroxycinnamoyl quinic acids and derivatives, organic acids, mono and diterpenoids and iridoids showed a significant increase after root inoculation with *Pbg*. Treatment of Artemisia with *Pbg* resulted in significant reduction in artemisinic acid while the relative levels of both dihydroartemisinin and artemisinic alcohol significantly increased. PC2 explained 16% of the total variance and corresponded to induced metabolites (cluster **3**) in response to *Pf* SS101 inoculation. Putative metabolite identification revealed that the amino acid arginine, fatty acyl glycoside blumenol glycoside and phenylpropanoid glycoside derivatives were induced in a *Pf* SS101-specific manner.

3.3.3 | Broccoli

Similar to Arabidopsis, inoculation of Broccoli roots with each of the three rhizobacterial strains resulted in substantial alteration of the shoot metabolome. From the 1908 detected metabolites, 933 (49%) were significantly different between at least two treatments. For this set of metabolites, HCA revealed eight distinct metabolite clusters of the host metabolome. PCA further showed that the metabolome of Broccoli seedlings inoculated with different rhizobacteria is clearly different from the control and from each other. The first three PCs explained 84% of the total variance (Figure 2c1). PC1, representing 47% of the total variance, was associated with metabolites that discriminate both the control and MB samples from the *Pbg* and *Pf* SS101 samples. These metabolites were either significantly increased or decreased in plants inoculated by *Pbg* or *Pf* SS101 (Figure 2c2 decreased cluster **3** and induced clusters **6** and **7**) that represent effective and ineffective partnerships with the host, respectively. The indole glucosinolate glucobrassicin also showed a significant increase in plants inoculated with *Pbg* and *Pf* SS101. PC2 explained 22% of the total variance and corresponded to metabolites that were either specifically altered in the *Pbg* or *Pf* SS101 treatments (Figure 2c1,c2 induced (clusters **8** [*Pf* SS101] and **9** [*Pbg*]) or reduced by *Pbg* inoculation [cluster **4**]). Metabolites that were specifically induced in the ineffective partnership between *Pf* SS101 and the host were dominated by flavonoids such as kaempferol, quercetin glycosides and glucosinolates including glucoibervirin, neoglucobrassicin and 4-methoxyglucobrassicin. Furthermore, several hydroxycinnamates conjugated or not with quinic acid, including chlorogenic acid (caffeoyl-quinic acid), coumaroyl quinic acid, sinapic acid and ferulic acid, were predominant in those metabolite clusters (clusters **7** and **8**). PC3 explained 15% of the total variation and corresponded to MB-induced metabolites represented in cluster **1** and induced metabolites by all three rhizobacteria in cluster **2**. Hexose 1-phosphate in cluster **1** showed a MB-specific increase. Meanwhile, some of the putatively annotated metabolites in cluster **2** including tryptophan, a precursor of indole glucosinolates, was reduced by all three rhizobacterial treatments.

3.4 | Metabolite signatures of Brassicaceae in effective and ineffective partnerships

The metabolome changes induced by the different rhizobacteria in the shoots of Arabidopsis and Broccoli were subjected to a comparative analysis as both plant species belong to the Brassicaceae family. Glucosinolates (GLS) are among the metabolites that showed alteration by rhizobacteria treatment. In Arabidopsis, the effective partnership with *Pf* SS101 enhanced the relative levels of aliphatic long-chain GLS such as glucohirsutin and 8-methylthiooctyl glucosinolate, whereas the ineffective partnership between *Pf* SS101 and Broccoli was characterized by an increase in the levels of indolic GLS (i.e., glucobrassicin, desulfoglucobrassicin, 4-methoxyglucobrassicin and neoglucobrassicin) and short-chain aliphatic GLS such as

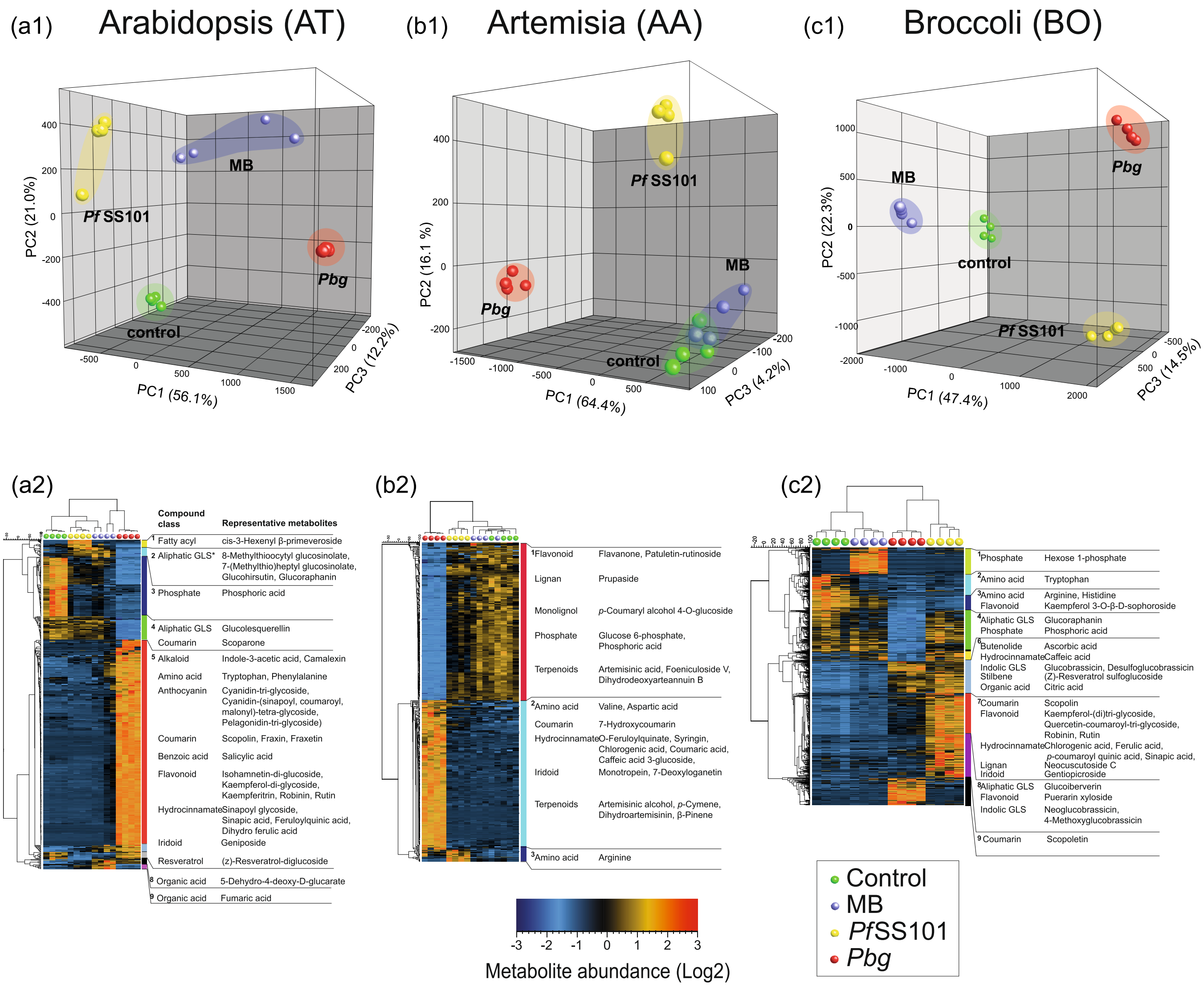

FIGURE 2 Rhizobacteria-mediated changes in the shoot metabolome. Shown are principal component analysis and hierarchical cluster analysis (HCA) plots based on differentially regulated semi-polar metabolites in the shoot of Arabidopsis (a1 and a2), Artemisia (b1 and b2) and Broccoli (c1 and c2) after root inoculation with three different rhizobacteria (*Pseudomonas fluorescens* SS101(PfSS101), Microbacterium sp EC8 [MB] and *Paraburkholderia graminis* mHS1 [Pbg]). *GLS, glucosinolate, **d, derivative. In the HCA, metabolite clusters are indicated by different colours and when none of the metabolites in a given cluster was annotated, the cluster number is omitted (clusters 6 and 7 in [a2] and cluster 5 in [b2]). For each treatment, four biological replicates were used. Each biological replicate is represented by a pooled sample of 10 Arabidopsis, 8 Artemisia and 5 Broccoli seedlings. [Color figure can be viewed at wileyonlinelibrary.com]

glucoibervirin. In contrast to the effective *Pf* SS101-Arabidopsis partnership, the ineffective *Pbg*-Arabidopsis partnership caused a drastic reduction of all detected aliphatic GLS, (i.e., glucohirsutin (8-methylsulfinyloctyl glucosinolate), glucolesquerellin (6-methylthio hexyl glucosinolate), 7-methylthioheptyl glucosinolate and 8-methylthiooctyl glucosinolate. In Broccoli, both the ineffective partnership with *Pf* SS101 as well as the effective partnership with *Pbg* caused significant increases of the indolic GLS glucobrassicin. Meanwhile, the effective MB-Arabidopsis partnership led to upregulation of glucohirsutin while this rhizobacterial strain barely influenced the level of GLS in Broccoli (Supporting Information: Tables S4 and S7). Considering their inconsistent accumulation patterns in effective and ineffective partnerships, GLS seem not to be appropriate plant metabolic markers for discriminating between effective and ineffective partnerships.

On the other hand, alteration of a particular branch of the phenylpropanoid pathway showed co-occurrence with growth promotion (effective partnership) or lack of growth promotion/growth reduction (ineffective partnership) in the different plant-rhizobacteria combinations tested. Higher accumulation of flavonoids was evident in the ineffective partnerships between Arabidopsis-*Pbg* and Broccoli-*Pf*SS101, while flavonoids showed no significant change in their abundance in the effective partnership between Arabidopsis-*Pf* SS101 (Figure 3 and

Supporting Information: Tables S4 and S7). Furthermore, in the ineffective partnerships between Arabidopsis-*Pbg*, indole-derived defensive compounds such as camalexin, β-D-glucopyranosyl indole-3-carboxylic acid and metabolites from the phenylpropanoid pathway (including anthocyanin and salicylic acid) showed higher accumulation (Figure 2a2, Supporting Information: Table S4 and Figure 3b). Similarly, the ineffective partnership between Broccoli and *Pf* SS101 resulted in a significant accumulation of flavonoids and other defensive metabolites (Figure 2c2, Supporting Information: Table S7). The accumulation of these stress/defense-related metabolites in the aforementioned ineffective partnerships suggests that both *Pbg* and *Pf* SS101 may be perceived as a biotic stressor by Arabidopsis and Broccoli, respectively (Figure 2a2,a3).

3.5 | Importance of the flavonoid pathway in plant growth promotion

In the ineffective rhizobacteria-plant partnerships, flavonoids showed considerably higher accumulation while they were not significantly changed or significantly reduced in effective and highly effective partnerships, respectively. Considering our results and other reports on the negative association between flavonoids and auxin transport, auxin distribution and turnover (Brown et al., 2001; Buer et al., 2013; Kuhn et al., 2017; Yin et al., 2014), we further investigated the effects of *Pbg* on growth of 12 isogenic homozygous Arabidopsis *transparent testa* (*tt*)-mutants (Appelhagen et al., 2014) disrupted in biosynthetic genes of different branches of the flavonoid pathway (Figure 4a). First, the inherent variation in shoot biomass of each of the 12

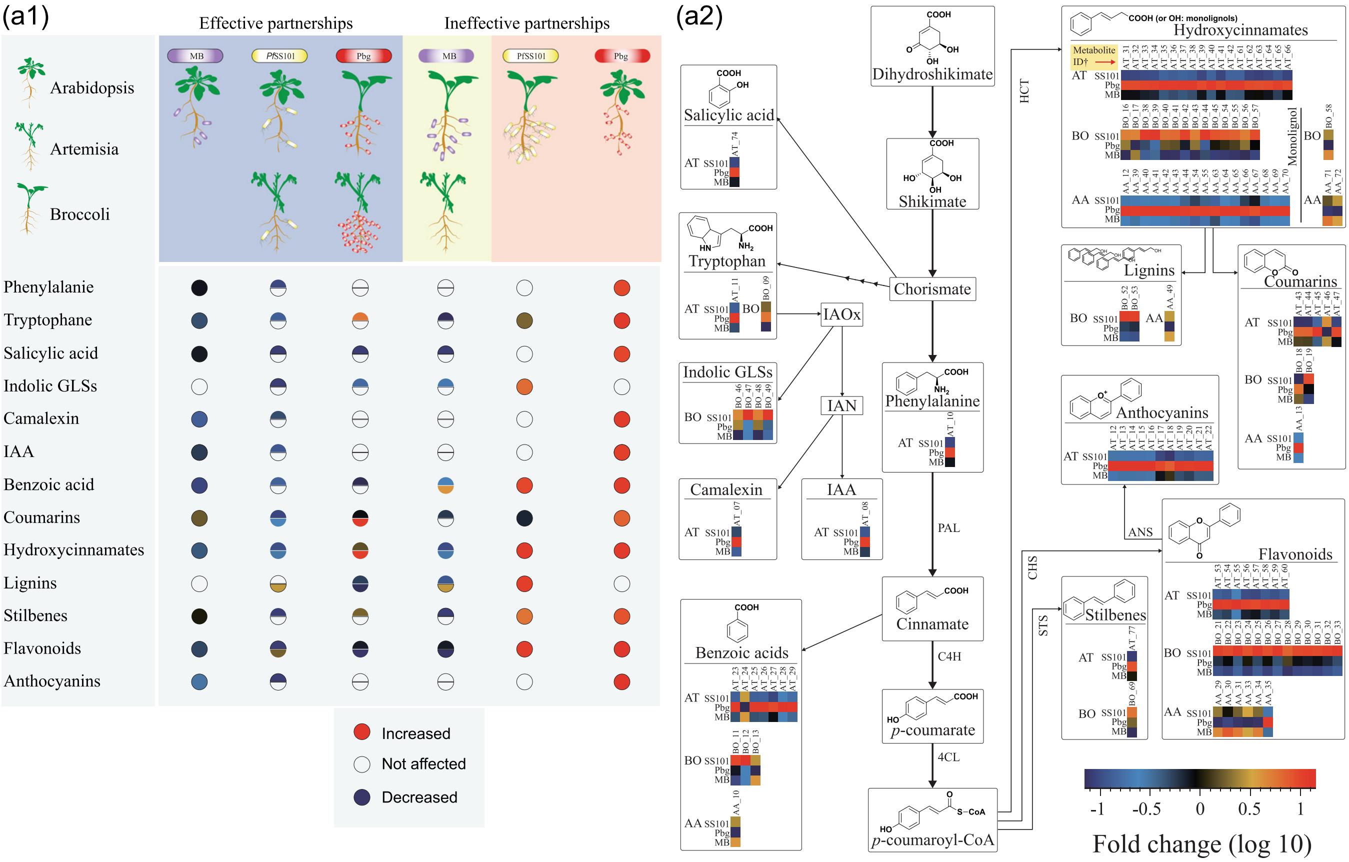

FIGURE 3 Rhizobacteria-host-dependent changes in phenylpropanoids. A simplified diagram representing changes in the shoot metabolome of three plant species (Arabidopsis [AT], Broccoli [BO] and Artemisia [AA]) in response to root tip inoculation with three rhizobacteria (Microbacterium EC8 (MB), *Pseudomonas fluorescens* SS101 (Pf SS101) and *Paraburkholderia graminis* mHS1(Pbg) (a1). Circles with different colours represent the patterns of changes in the metabolite subclass of the phenylpropanoid pathway and the intensity of the colours corresponds to the relative fold changes. The pattern of root colonization of the rhizobacteria for the different plants is shown in the diagram. Experimentally generated figures of the root colonization are provided in Supporting Information: Table S2. A simplified phenylpropanoid pathway showing the relationship between the significantly changed metabolites in the biosynthesis route (a2). The metabolites corresponding to the different branches of the phenylpropanoid pathway are indicated by the metabolite ID corresponding to each species and their level of accumulation is indicated by the scaled fold change corresponding to the green and red boxes for each of the metabolites. For detailed information on the identity of the individual metabolites, consult the Supporting Information: Tables S4, S7 and S8. IAOx (indole-3-acetaldoxime), IAN (indole-3-acetonitrile), PAL (Phenylalanine ammonia-lyase), C4H (Cinnamate 4-hydroxylase), 4CL (4-coumarate-CoA ligase), CHS (Chalcone synthase), HCT (hydroxycinnamoyl-CoA shikimate/quinate hydroxycinnamoyl transferase) and STS (Stilbene synthase). [Color figure can be viewed at wileyonlinelibrary.com]

mutant lines and wild-type (WT) Col-0 was assessed in absence of *Pbg*. Second, the effect of *Pbg* on growth of these 12 mutants and Col-0 was assessed by calculating the percent change in shoot biomass relative to the biomass of the respective nontreated mutant line or WT. Both measures were subjected to analysis of variance (ANOVA) by considering the 'genotype' as a factor and root biomass and percent change in shoot biomass as dependent variables.

In absence of *Pbg*, we observed significant variation in shoot biomass among the *tt*-mutants and between several of the *tt*-mutants and WT Col-0 (Figures 4b,c and Supporting Information: Table S5). Mutants disrupted in the initial steps of the flavonoid pathway (*tt*-4 and *tt*-6) showed similar shoot biomass as WT Col-0 and higher shoot biomass than many of the mutants with genes disrupted in the downstream steps of the pathway, especially mutants *tds*4, *aha*10 and *tt*10 that are associated with the biosynthesis of flavan-3-ols (proanthocyanidns (PA)) (Figure 4c).

Root tip inoculation with *Pbg* led to significant changes in shoot fresh biomass between the 12 mutants (Figure 4c and Supporting

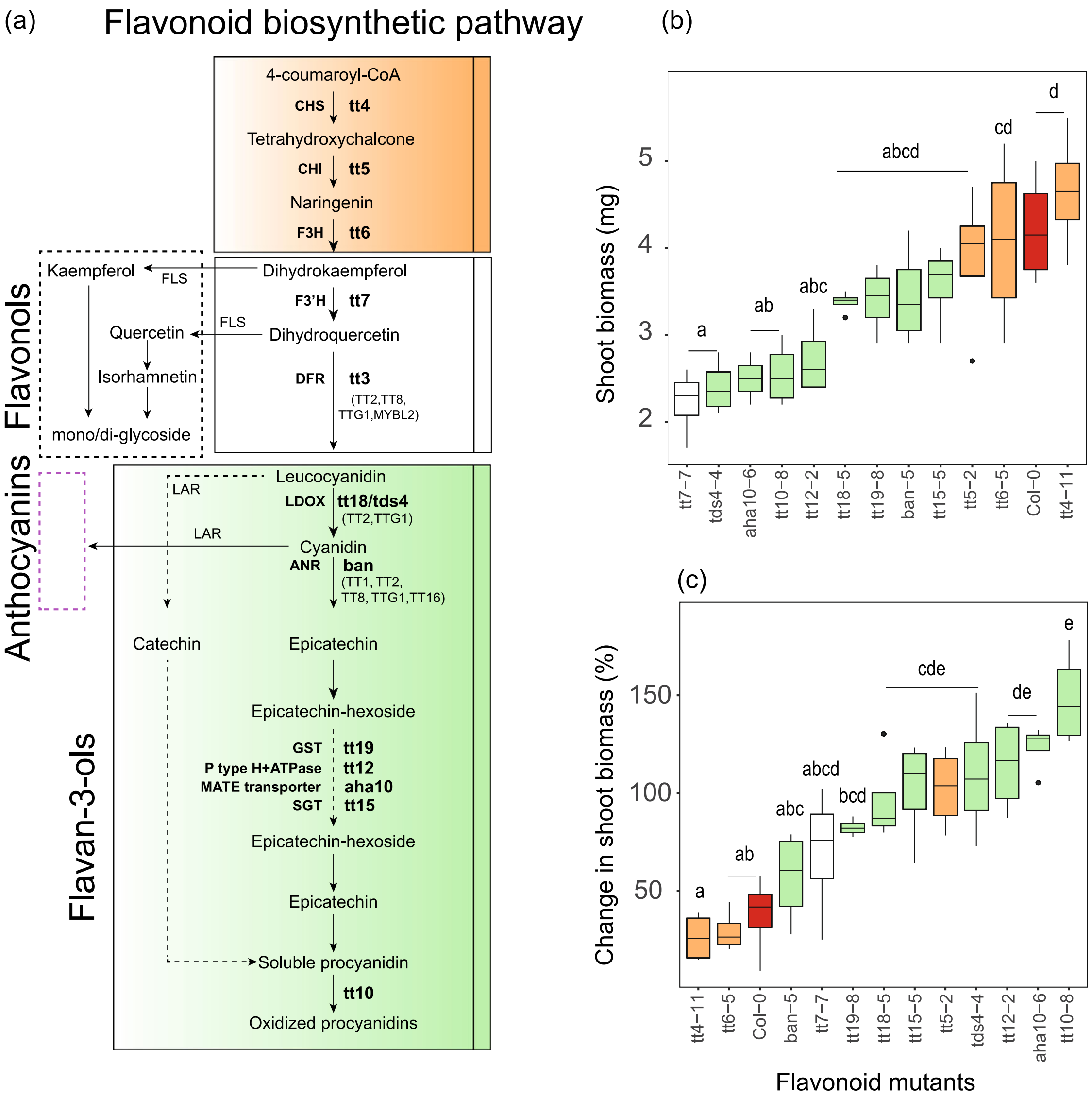

FIGURE 4 Role of flavonoids in rhizobacteria-mediated growth promotion. A simplified flavonoid pathway representing the different branches including flavonols, anthocyanin and the proanthocyanidins (flavan-3-ols). The early stages of the pathway are depicted by the orange box followed by first intermediates of the flavonol pathways in white box and the intermediates for the anthocyanin and proanthocyanidin biosynthesis in the green box. TT1, TT2, TT8, TTG1 and TT16 loci encode regulatory proteins (transcription factors). CHS, chalcone synthase; CHI, chalcone isomerase; F3H, flavone 3 hydroxylase; F3′H, flavone 3′ hydroxylase; DFR, dihydroflavonol reductase; FLS, flavonol synthase, GST, gluthatione S-transferase and SGT, UDPglucose:sterol glucosyltransferase (a). The inherent variation in shoot fresh biomass accumulation between the tt-mutants and the wild-type Col-0 (b). The percent change in shoot fresh biomass of the tt-mutants and the wild type Col-0 after 14 days of inoculation with Pbg (c). Data are mean ± standard error (SE); ($n = 4$ biological replicates). A biological replicate is represented by 10 seedlings grown in an agar plate. Means sharing the same letter are not significantly different based on one-way analysis of variance (Tukey, $p < 0.05$). [Color figure can be viewed at wileyonlinelibrary.com]

Information: Table S6). It should be noted that in contrast to the previous assays, *Pbg* did cause a slight growth-promotion of Col-0 in these mutant assays. *Pbg*-treated seedlings showed a consistent shoot fresh biomass (~5.5 mg per plant) across all assays, but the nontreated Col-0 plants had significantly lower fresh biomass in these latter assays as compared to the previous assays, explaining the slight growth-promoting effect in the latter. The cause of the reduced vigor of nontreated plants in these assays is not fully clear but is most likely due to the difference in growth period (14 days instead of 11 days) and/or the use of a different Col-0 seed batch in the latter assays. Nevertheless, what is evident and consistent between all assays is that plants treated with *Pbg* showed clear signs of stress as exemplified by elevated anthocyanin levels in the leaves (Supporting Information: Figure S4). This response aligns well with an ineffective partnership. Interestingly, *Pbg* had the strongest growth-promoting effect on mutants affected in the downstream part of the flavonoid pathway, particularly on mutants in the PA branch (*tt*10-8, *aha*10-6, *tt*12-2, *tds*−4, *tt*15-5 and *tt*18-5) (Figure 4c). The *tt*-7 mutant that accumulates kaempferol-derived flavonols showed inherently the lowest shoot biomass accumulation (Figure 4c) and root inoculation of this mutant with *Pbg* had no significant growth-promoting effect as compared to the WT (Figure 4c). Collectively, these results indicate that the PA branch plays a key role in *Pbg*-mediated growth promotion.

4 | DISCUSSION

Over the past decades, several studies indicated that strains of various rhizobacterial species can promote plant growth, induce systemic resistance against pathogens and phytophagous insects and can alter plant secondary metabolism (Etalo et al., 2018; Hu et al., 2018; Jeon et al., 2021; van de Mortel et al., 2012; Stringlis, Yu, et al., 2018). Our results confirm and extend results obtained in previous studies (Barriuso et al., 2008; Cordovez et al., 2018; van de Mortel et al., 2012; Walker et al., 2011) and provide, for the first time, new insights into global metabolome changes and specific plant metabolic signatures of effective and ineffective partnerships between rhizobacteria and their host plant.

4.1 | Finding the right rhizobacterial partner is key for plant growth promotion

Of the three tested rhizobacterial genera, none of the strains showed growth-promoting effects for all three plant species, indicating specificity in rhizobacteria-plant interactions (Figure 1). For example, *Pbg* established an effective partnership with Artemisia and Broccoli, whereas interaction with Arabidopsis was deleterious given the significant reduction in biomass and the accumulation of stress-related dark-purple anthocyanins in the leaves (Figure 1a). Even when an effective partnership between rhizobacteria and the host took place, the extent of growth promotion can significantly differ as shown by the partnership between *Pbg* and Artemisia (~500%) and Broccoli (~50%). The temporal analyses of the rhizobacteria-host interactions also demonstrated that tshe establishment of an effective partnership was characterized by early and sustained induction of growth promotion as was shown for the interaction of *Pbg* with Artemisia and Broccoli (Figure 1e,f). The differential growth response of the three plant species to *Pbg* inoculation exemplifies the importance of the right partnership for growth promotion.

4.2 | Root colonization by rhizobacteria showed no clear association with growth promotion

It is widely known that plant growth-promoting rhizobacteria must colonize the rhizosphere of the host plant to a specific threshold density to be beneficial (Benizri et al., 2001). The establishment of high population densities of PGPR on roots has been proposed as a prerequisite of plant growth promotion. This is exemplified in our results by the lack of phenotypic responses of Artemisia to MB inoculation (Figure 3a1 and Supporting Information: Figure S2). However, our results also indicated that high rhizosphere population densities of the introduced strains can be associated with either growth promotion or growth reduction as was seen for the combination of *Pbg* with Artemisia (growth promotion) and *Pbg* with Arabidopsis (growth reduction) (Supporting Information: Figures S2a2,a1, respectively).

4.3 | Flavonoids: A common signature of rhizobacteria-mediated plant growth promotion

Our results showed that one of the most distinctive metabolic signatures between effective and ineffective partnerships is the differential regulation of the flavonoid pathway. In effective partnerships, metabolites from this pathway were either suppressed or showed only a slight accumulation. In ineffective partnerships, metabolites from this pathway were highly induced in the shoot (Figures 2 and 3). Of all rhizobacteria-plant combinations, the *Pbg*-Artemisia combination can be considered as a highly-effective partnership in terms of growth promotion and was hallmarked by a substantial alteration of the host metabolome (Figure 1 and Figure 2c1,2). This ‘rewiring’ of the Artemisia metabolome primarily involved the accumulation of hydroxycinnamates and suppression of other phenolic compounds such as flavonoids and benzoic acid derivatives (Figure 3a1,2 and Supporting Information: Table S8). This phenomenon might be the result of the competition for the common precursor *P*-coumaroyl CoA between hydroxycinnamoyl transferase (HCT) and chalcone synthase (CHS), key enzymes involved in the biosynthesis of hydroxycinnamates (monolignols) and flavonoids, respectively (Figure 3a2 and Supporting Information: Table S6).

Similar to the ineffective partnerships of *Pbg*-Arabidopsis or *Pf* SS101-Broccoli, Besseau et al. (2007) showed that the HCT-mutants displayed reduced growth and a concomitant accumulation of flavonoids of mainly kaempferol derivatives. Accumulation of flavonoid glycosides in Arabidopsis are reported to affect auxin transport (Besseau et al., 2007), distribution and turnover (Kuhn et al., 2016), thereby affecting plant growth. Besseau et al. (2007); further showed that suppression of flavonoid production via CHS silencing, restored auxin transport and normal development of HCT-deficient plants. Another interesting *Pbg*-induced chemotype we observed in Arabidopsis was the accumulation of metabolites derived from the indole pathways such as IAA and camalexin. The accumulation of auxin in the aerial part of the plant might suggest that rootward transport of auxin is inhibited in Arabidopsis colonized by *Pbg*. Flavonoids were implicated as endogenous metabolites that reduce the basipetal transport of auxin (Peer et al., 2004; Santelia et al., 2008). Interestingly, the ineffective partnership between *Pf* SS101 and Broccoli was characterized by the accumulation of indolic glucosinolates while IAA and camalexin were not detected in the samples. In contrary to Besseau et al. (2007), Li et al. (2010) suggested that growth reduction associated with lignin biosynthesis in Arabidopsis is independent of flavonoids. Other studies also showed that the accumulation of flavonoids either increases plant biomass (Sharma et al., 2016) or does not lead to a growth penalty (Nakabayashi et al., 2014), making the association between growth and flavonoids debatable. Elucidation of the role of a class of metabolites in plant growth by targeting a gene at branching points of different biosynthetic pathways or by targeting transcription factors that potentially involve in multiple metabolic pathways will have spillover effect and could jeopardize our attempt to establish relationship between a given metabolite class and plant growth phenotype. Hence, in our study, we used specific Arabidopsis mutants and focused on the role of the flavonoid pathway and its different branches in rhizobacteria-mediated plant growth promotion.

4.4 | The PA branch of the flavonoid pathway affects rhizobacteria-mediated growth promotion in Arabidopsis

Considering our results and other reports on the negative impact of flavonoids on auxin transport, auxin distribution and turnover (Besseau et al., 2007; Brown et al., 2001; Buer et al., 2013; Kuhn et al., 2011, 2016; Murphy et al., 2000; Santelia et al., 2008), we investigated if *Pbg* can establish an effective partnership with Arabidopsis *transparent testa* (*tt*) mutants that harbour mutations in biosynthetic and transport genes along the main trunk route of the flavonoid pathway. Before assessing the response of the *tt*-mutants to *Pbg*, we evaluated their inherent variation in biomass accumulation. These 12 mutants showed significant variation in biomass accumulation. In general, mutants in the downstream steps of the flavonoid pathway showed reduced shoot biomass when compared to mutants from the upstream steps of the pathway (*tt4*, *tt5* and *tt6*) and the WT (Figure 4a,b). The upstream mutants produce no detectable level of flavonols that are often implicated to interfere with auxin transport and turnover (Bowerman et al., 2012). However, that did not lead to growth promotion in these mutants. The *tt7* mutant that accumulates kaempferol-derived flavonols (Routaboul et al., 2006) showed the lowest shoot biomass accumulation (Figure 4b) and when treated with *Pbg* showed no significant difference in shoot biomass from the WT (Figure 4c). Interestingly, both the ineffective partnerships between Arabidopsis-*Pbg* and Broccoli-*Pf*SS101 exhibited high accumulation of kaempferol-derived flavonols (Figure 2a2,b2). In Arabidopsis, kaempferol diglycosides are reported to act as an endogenous polar auxin transport inhibitor (Buer & Muday 2004; Kuhn et al., 2016, 2017; Peer et al., 2004; Yin et al., 2014). This may suggest that kaempferol-derived flavonols could negatively influence the inherent growth of Arabidopsis and also potentially compromise its responsiveness to *Pbg*.

From the early steps of the flavonoid pathway, mutants *tt4*, *tt5* and *tt6* are defective in the biosynthesis of the three main branches of the flavonoid pathway such as flavonols, anthocyanins and PA (Bowerman et al., 2012; Lepiniec et al., 2006). Of the three mutants, *tt4* and *tt6* responded the least to *Pbg* in terms of shoot biomass accumulation suggesting that some group of flavonoids might be required for *Pbg*-mediated growth promotion. Although the *tt5* mutant was expected to behave similarly to *tt4* and *tt6*, it showed a significant increase in shoot biomass accumulation upon treatment with *Pbg* probably owing to its 'leaky' phenotype (Peer et al., 2001). Shutting down the flavonoid pathway by blocking genes involved in the early steps of biosynthesis (*tt4/5/6*) was expected to have a similar growth-promoting effect. Possibly, other pleiotropic effects of these mutations may have dampened and differentiated the effects of *Pbg* on these mutants. For example, tt4/5/6 mutations have been shown to lead to the accumulation of different precursors with a putative spill-over effect on other metabolite pathways, such as sinapate-derived metabolites and p-coumarate-derived choline esters (Böttcher et al., 2008; Xuan et al., 2018; Yonekura-Sakakibara et al., 2008). To resolve if these spill-over effects have interfered with the *Pbg*-response in these mutants will require future studies with other combinations of mutations. Regarding the proposed 'leaky' phenotype of the *tt5* mutant, Peer et al. (2001) detected chalcone and a flavonone skeleton in *tt5* mutants and suggested spontaneous isomerization of naringenin chalcone to naringenin may have resulted in the formation of a flavonone structure in the *tt5*-1 mutant, an allelic variant of *tt5*-2 used in our study. Similarly, Shirley et al. (1995) and Routaboul et al. (2006) also reported reduced levels of flavonols in the *tt5* mutant.

Mutants from the downstream branches of the flavonoid pathway defective in anthocyanin (*tt18*, *tds4*) and PA biosynthesis (*tt18*, *tds4*, *tt15*, *tt12*, *aha10* and *tt10*) established effective partnership with *Pbg* leading to significant increases in shoot biomass (Figure 4c). The role of anthocyanin can be excluded in the establishment of effective partnership as the *ban* mutant that accumulates anthocyanin at the expense of PA (Devic et al., 1999; Xie et al., 2003) showed no significant influence on the growth phenotype. Similarly, the *tt7* that does not accumulate anthocyanin showed no significant growth promotion when treated with *Pbg*. Hence, the influence of *tt*18 and *tds*4 on the establishment of effective partnerships could be due to their influence on the PA pathway.

Among the PA mutants, the *tt*12 gene encodes a transporter that is homologous to the multidrug and toxic compound extrusion (MATE) secondary transporter (Marinova et al., 2007), the *aha*10 gene encodes a H^+-ATPse that is also involved in PA metabolism (Baxter et al., 2005) and *tt*15 encodes the UDP-Glc:sterol glycosyltransferase UGT8B (DeBolt et al., 2009). The *tt*10 gene is involved in the formation of polymeric pigments from epicatechin and may catalyze the oxidative browning of colourless PAs (Pourcel et al., 2005). *Pbg* had the highest growth-promoting effect on the *tt*10 mutant that was reported to accumulate epicatechin (CE) and procyanidin polymers and soluble PA but lacks oxidized PA (Pourcel et al., 2005). Mutant *tt*15 showed reduced PA and oxidized PA, cyanidin and quercetin (Focks et al., 1999; Routaboul et al., 2012), *tt*12 revealed the absence of CE, PA, oxidized PA and reduction of the major flavonol quercetin-3-*o*-rhamnoside (Marinova et al., 2007) and *aha*10 accumulates CE and shows highly reduced PA and oxidized PA (Baxter et al., 2005). When evaluated together, the *tt*15, *tt*12 and *aha*10 mutants lack or have a highly reduced PA and a concomitant reduction of oxidized PA. The *tds*4 and *tt*18 mutants that established effective partnership with *Pbg* are reported to lack or have highly reduced anthocyanin levels, have reduced CE, highly reduced PA and lack oxidized PA. Hence, the common denominator of all Arabidopsis *transparent testa* (*tt*) mutants that established an effective partnership with *Pbg* is the absence of oxidized PA (tannins). In conclusion, our results indicate that the flavonoid pathway is a prime target of rhizobacteria and various branches of this pathway can have different impacts on the inherent growth and responsiveness of Arabidopsis to growth-promoting rhizobacteria. Based on these results, we postulate that kaempferol-derived flavonols and the oxidized products of PA can negatively influence rhizobacteria-mediated plant growth promotion.

4.5 | Rhizobacteria as agents to enhance high-value natural products in plants

Beyond assessing the co-occurrence of specific metabolites associated with growth promotion in different plant-bacteria interactions, our result also revealed that the three different rhizobacterial genera can boost nutritionally and/or pharmaceutically important high-value natural plant compounds (HVPC). The list of various putative HVPC is summarized in Supporting Information: Table S9. Among these, flavonoid glycosides induced in the ineffective partnership between *Pbg* and Arabidopsis are considered vital phytochemicals in diets and are of great interest due to their diverse bioactivities (Xiao et al., 2016). Similarly, glucosinolates in Brassica species (Traka 2016), hydroxycinnamic acid derivatives (Alam et al., 2016) and dihydroartemisinin in Artemisia (Tilley et al., 2016) are potential HPVC. In effective partnerships, the increase in these compounds is even more pronounced when we consider the increase in host biomass due to rhizobacteria inoculation. A typical example for this is the *Pbg*-Artemisia combination that resulted in fivefold increase in host biomass and up to threefold increase in both artemisinic alcohol and dihydroartemisinin per unit fresh tissue biomass. Hence, the use of rhizobacteria may be considered as a simple and generic approach to boost economically or pharmaceutically interesting plant metabolites.

ACKNOWLEDGEMENTS

Artemisia F1seed and Broccoli seeds were kindly provided by the Department of Biology, University of York, York, UK, and Bejo seed company (Trambaan1, 1749 CZ Warmenhuizen, The Netherlands), respectively. We are grateful to Bert Schipper and Henriëtte Vaneekelen for their help with LC-MS analysis and preprocessing of metabolomics data. Part of this project was supported by the Korean government scholarship program of the National Institute for International Education (NIIED).

CONFLICT OF INTEREST

The authors declare no conflict of interest.

DATA AVAILABILITY STATEMENT

The raw data that support the findings of this study are available from the corresponding authors upon reasonable request.

ORCID

Desalegn W. Etalo http://orcid.org/0000-0002-8836-5113

REFERENCES

Alam, M.A., Subhan, N., Hossain, H., Hossain, M., Reza, H.M., Rahman, M.M. et al. (2016) Hydroxycinnamic acid derivatives: a potential class of natural compounds for the management of lipid metabolism and obesity. *Nutrition & Metabolism*, 13, 27.

Appelhagen, I., Thiedig, K., Nordholt, N., Schmidt, N., Huep, G., Sagasser, M. et al. (2014) Update on transparent testa mutants from *Arabidopsis thaliana*: characterisation of new alleles from an isogenic collection. *Planta*, 240, 955–970.

Barriuso, J., Ramos Solano, B., Fray, R.G., Cámara, M., Hartmann, A. & Gutiérrez Mañero, F.J. (2008) Transgenic tomato plants alter quorum sensing in plant growth-promoting rhizobacteria. *Plant Biotechnology Journal*, 6, 442–452.

Baxter, I.R., Young, J.C., Armstrong, G., Foster, N., Bogenschutz, N., Cordova, T. et al. (2005) A plasma membrane H+-ATPase is required for the formation of proanthocyanidins in the seed coat endothelium of *Arabidopsis thaliana*. *Proceedings of the National Academy of Sciences*, 102, 2649–2654.

Benizri, E., Baudoin, E. & Guckert, A. (2001) Root colonization by inoculated plant Growth-Promoting rhizobacteria. *Biocontrol Science and Technology*, 11, 557–574.

Besseau, S., Hoffmann, L., Geoffroy, P., Lapierre, C., Pollet, B. & Legrand, M. (2007) Flavonoid accumulation in arabidopsis repressed in lignin synthesis affects auxin transport and plant growth. *The Plant Cell*, 19, 148–162.

Böttcher, C., von Roepenack-Lahaye, E., Schmidt, J., Schmotz, C., Neumann, S., Scheel, D. et al. (2008) Metabolome analysis of biosynthetic mutants reveals a diversity of metabolic changes and allows identification of a large number of new compounds in arabidopsis. *Plant Physiology*, 147, 2107–2120.

Bowerman, P.A., Ramirez, M.V., Price, M.B., Helm, R.F. & Winkel, B.S. (2012) Analysis of T-DNA alleles of flavonoid biosynthesis genes in Arabidopsis ecotype Columbia. *BMC Research Notes*, 5, 485.

Brown, D.E., Rashotte, A.M., Murphy, A.S., Normanly, J., Tague, B.W., Peer, W.A. et al. (2001) Flavonoids act as negative regulators of auxin transport in vivo in arabidopsis. *Plant Physiology*, 126, 524–535.

Buer, C.S., Kordbacheh, F., Truong, T.T., Hocart, C.H. & Djordjevic, M.A. (2013) Alteration of flavonoid accumulation patterns in transparent testa mutants disturbs auxin transport, gravity responses, and imparts long-term effects on root and shoot architecture. *Planta*, 238, 171–189.

Buer, C.S. & Muday, G.K. (2004) The transparent testa4 mutation prevents flavonoid synthesis and alters auxin transport and the response of arabidopsis roots to gravity and light. *The Plant Cell*, 16, 1191–1205.

Carrión, V.J., Cordovez, V., Tyc, O., Etalo, D.W., de Bruijn, I., de Jager, V.C.L. et al. (2018) Involvement of Burkholderiaceae and sulfurous volatiles in disease-suppressive soils. *The ISME Journal*, 12, 2307–2321.

Chamam, A., Sanguin, H., Bellvert, F., Meiffren, G., Comte, G., Wisniewski-Dyé, F. et al. (2013) Plant secondary metabolite profiling evidences strain-dependent effect in the Azospirillum–*Oryza sativa* association. *Phytochemistry*, 87, 65–77.

Cheng, X., Etalo, D.W., van de Mortel, J.E., Dekkers, E., Nguyen, L., Medema, M.H. et al. (2017) Genome-wide analysis of bacterial determinants of plant growth promotion and induced systemic resistance by *Pseudomonas fluorescens*. *Environmental Microbiology*, 19, 4638–4656.

Cordovez, V., Schop, S., Hordijk, K., Dupré de Boulois, H., Coppens, F., Hanssen, I. et al. (2018) Priming of plant growth promotion by volatiles of root-associated microbacterium spp. *Applied and Environmental Microbiology*, 84, e01865–18.

De Souza, J.T., De Boer, M., De Waard, P., Van Beek, T.A. & Raaijmakers, J.M. (2003) Biochemical, genetic, and zoosporicidal properties of cyclic lipopeptide surfactants produced by *Pseudomonas fluorescens*. *Applied and Environmental Microbiology*, 69, 7161–7172.

De Vleesschauwer, D. & Höfte, M. (2009) Chapter 6 Rhizobacteria-Induced Systemic Resistance. In Advances in Botanical Research. *Advances in Botanical Research*. Academic Press. pp. 223–281.

De Vos, R.C., Moco, S., Lommen, A., Keurentjes, J.J., Bino, R.J. & Hall, R.D. (2007) Untargeted large-scale plant metabolomics using liquid chromatography coupled to mass spectrometry. *Nature Protocols*, 2, 778–791.

DeBolt, S., Scheible, W.-R., Schrick, K., Auer, M., Beisson, F., Bischoff, V. et al. (2009) Mutations in UDP-glucose:sterol glucosyltransferase in arabidopsis cause transparent testa phenotype and suberization defect in seeds. *Plant Physiology*, 151, 78–87.

Devic, M., Guilleminot, J., Debeaujon, I., Bechtold, N., Bensaude, E., Koornneef, M. et al. (1999) The BANYULS gene encodes a DFR-like protein and is a marker of early seed coat development. *The Plant Journal*, 19, 387–398.

Etalo, D.W., Jeon, J.-S. & Raaijmakers, J.M. (2018) Modulation of plant chemistry by beneficial root microbiota. *Natural Product Reports*, 35, 398–409.

Focks, N., Sagasser, M., Weisshaar, B. & Benning, C. (1999) Characterization of tt15, a novel transparent testa mutant of *Arabidopsis thaliana* (L.) Heynh. *Planta*, 208, 352–357.

Hu, L., Robert, C.A.M., Cadot, S., Zhang, X., Ye, M., Li, B. et al. (2018) Root exudate metabolites drive plant-soil feedbacks on growth and defense by shaping the rhizosphere microbiota. *Nature Communications*, 9, 2738.

Jeon, J.-S., Carreno-Quintero, N., van Eekelen, H.D.L.M., De Vos, R.C.H., Raaijmakers, J.M. & Etalo, D.W. (2021) Impact of root-associated strains of three Paraburkholderia species on primary and secondary metabolism of *Brassica oleracea*. *Scientific Reports*, 11, 2781.

Kuhn, B.M., Errafi, S., Bucher, R., Dobrev, P., Geisler, M., Bigler, L. et al. (2016) 7-Rhamnosylated flavonols modulate homeostasis of the plant hormone auxin and affect plant development. *The Journal of Biological Chemistry*, 291, 5385–5395.

Kuhn, B.M., Geisler, M., Bigler, L. & Ringli, C. (2011) Flavonols accumulate asymmetrically and affect auxin transport in arabidopsis. *Plant Physiology*, 156, 585–595.

Kuhn, B.M., Nodzyński, T., Errafi, S., Bucher, R., Gupta, S., Aryal, B. et al. (2017) Flavonol-induced changes in PIN2 polarity and auxin transport in the *Arabidopsis thaliana* rol1-2 mutant require phosphatase activity. *Scientific Reports*, 7, 41906.

Lambers, H., Mougel, C., Jaillard, B. & Hinsinger, P. (2009) Plant-microbe-soil interactions in the rhizosphere: an evolutionary perspective. *Plant and Soil*, 321, 83–115.

Lepiniec, L., Debeaujon, I., Routaboul, J.-M., Baudry, A., Pourcel, L., Nesi, N. et al. (2006) Genetics and biochemistry of seed flavonoids. *Annual review of plant biology*, 57, 405–430.

Li, X., Bonawitz, N.D., Weng, J.-K. & Chapple, C. (2010) The growth reduction associated with repressed lignin biosynthesis in *Arabidopsis thaliana* is independent of Flavonoids[C]. *The Plant Cell*, 22, 1620–1632.

Lommen, A. (2009) MetAlign: interface-driven, versatile metabolomics tool for hyphenated full-scan mass spectrometry data preprocessing. *Analytical Chemistry*, 81, 3079–3086.

van Loon, L.C., Bakker, P.A. & Pieterse, C.M. (1998) Systemic resistance induced by rhizosphere bacteria. *Annual Review of Phytopathology*, 36, 453–483.

Lugtenberg, B. & Kamilova, F. (2009) Plant-growth-promoting Rhizobacteria. *Annual Review of Microbiology*, 63, 541–556.

Marinova, K., Pourcel, L., Weder, B., Schwarz, M., Barron, D., Routaboul, J.-M. et al. (2007) The arabidopsis MATE transporter TT12 acts as a vacuolar flavonoid/H+-antiporter active in proanthocyanidin-accumulating cells of the seed coat. *The Plant Cell*, 19, 2023–2038.

Mendes, R., Kruijt, M., de Bruijn, I., Dekkers, E., van der Voort, M., Schneider, J.H. et al. (2011) Deciphering the rhizosphere microbiome for disease-suppressive bacteria. *Science*, 332, 1097–1100.

Mishra, R.P.N., Singh, R.K., Jaiswal, H.K., Kumar, V. & Maurya, S. (2006) Rhizobium-Mediated induction of phenolics and plant growth promotion in rice (*Oryza sativa* L.). *Current Microbiology*, 52, 383–389.

van de Mortel, J.E., de Vos, R.C.H., Dekkers, E., Pineda, A., Guillod, L., Bouwmeester, K. et al. (2012) Metabolic and transcriptomic changes induced in arabidopsis by the rhizobacterium *Pseudomonas fluorescens*. *Plant Physiology*, 160, 2173–2188.

Murphy, A., Peer, W.A. & Taiz, L. (2000) Regulation of auxin transport by aminopeptidases and endogenous flavonoids. *Planta*, 211, 315–324.

Nakabayashi, R., Yonekura-Sakakibara, K., Urano, K., Suzuki, M., Yamada, Y., Nishizawa, T. et al. (2014) Enhancement of oxidative and drought tolerance in Arabidopsis by overaccumulation of antioxidant flavonoids. *The Plant Journal*, 77, 367–379.

Ostonen, I., Lõhmus, K., Helmisaari, H.-S., Truu, J. & Meel, S. (2007) Fine root morphological adaptations in Scots pine, Norway spruce and silver birch along a latitudinal gradient in boreal forests. *Tree Physiology*, 27, 1627–1634.

Peer, W.A., Bandyopadhyay, A., Blakeslee, J.J., Makam, S.N., Chen, R.J., Masson, P.H. et al. (2004) Variation in expression and protein localization of the PIN family of auxin efflux facilitator proteins in flavonoid mutants with altered auxin transport in *Arabidopsis thaliana*. *The Plant Cell*, 16, 1898–1911.

Peer, W.A., Brown, D.E., Tague, B.W., Muday, G.K., Taiz, L. & Murphy, A.S. (2001) Flavonoid accumulation patterns of transparent testa mutants of arabidopsis. *Plant Physiology*, 126, 536–548.

Pineda, A., Zheng, S.-J., van Loon, J.J.A., Pieterse, C.M.J. & Dicke, M. (2010) Helping plants to deal with insects: the role of beneficial soil-borne microbes. *Trends in Plant Science*, 15, 507–514.

Pourcel, L., Routaboul, J.-M., Kerhoas, L., Caboche, M., Lepiniec, L. & Debeaujon, I. (2005) TRANSPARENT TESTA10 encodes a Laccase-Like enzyme involved in oxidative polymerization of flavonoids in arabidopsis seed coat. *The Plant Cell*, 17, 2966–2980.

Raaijmakers, J.M., Paulitz, T.C., Steinberg, C., Alabouvette, C. & Moënne-Loccoz, Y. (2009) The rhizosphere: a playground and battlefield for soilborne pathogens and beneficial microorganisms. *Plant and Soil*, 321, 341–361.

Ridder, L., van der Hooft, J.J.J., Verhoeven, S., de Vos, R.C.H., Bino, R.J. & Vervoort, J. (2013) Automatic chemical structure annotation of an LC–MSn based metabolic profile from green tea. *Analytical Chemistry*, 85, 6033–6040.

Routaboul, J.-M., Kerhoas, L., Debeaujon, I., Pourcel, L., Caboche, M., Einhorn, J. et al. (2006) Flavonoid diversity and biosynthesis in seed of *Arabidopsis thaliana*. *Planta*, 224, 96–107.

Routaboul, J.-M., Dubos, C., Beck, G., Marquis, C., Bidzinski, P., Loudet, O. et al. (2012) Metabolite profiling and quantitative genetics of natural variation for flavonoids in Arabidopsis. *Journal of Experimental Botany*, 63, 3749–3764.

Santelia, D., Henrichs, S., Vincenzetti, V., Sauer, M., Bigler, L., Klein, M. et al. (2008) Flavonoids redirect PIN-mediated polar auxin fluxes during root gravitropic responses. *The Journal of Biological Chemistry*, 283, 31218–31226.

Sharma, D., Tiwari, M., Pandey, A., Bhatia, C., Sharma, A. & Trivedi, P.K. (2016) MicroRNA858 is a potential regulator of phenylpropanoid pathway and plant development. *Plant Physiology*, 171, 944–959.

Shirley, B.W., Kubasek, W.L., Storz, G., Bruggemann, E., Koornneef, M., Ausubel, F.M. et al. (1995) Analysis of Arabidopsis mutants deficient in flavonoid biosynthesis. *The Plant Journal: For Cell and Molecular Biology*, 8, 659–671.

Stringlis, I.A., Yu, K., Feussner, K., Jonge, R., de, Bentum, S.V., Verk, M.C.V. et al. (2018) MYB72-dependent coumarin exudation shapes root microbiome assembly to promote plant health. *Proceedings of the National Academy of Sciences*, 115, E5213–E5222.

Stringlis, I.A., Zhang, H., Pieterse, C.M.J., Bolton, M.D. & de Jonge, R. (2018) Microbial small molecules—weapons of plant subversion. *Natural Product Reports*, 35, 410–433.

Tikunov, Y.M., Laptenok, S., Hall, R.D., Bovy, A. & de Vos, R.C.H. (2012) MSClust: a tool for unsupervised mass spectra extraction of chromatography-mass spectrometry ion-wise aligned data. *Metabolomics*, 8, 714–718.

Tilley, L., Straimer, J., Gnädig, N.F., Ralph, S.A. & Fidock, D.A. (2016) Artemisinin action and resistance in *Plasmodium falciparum*. *Trends In Parasitology*, 32, 682–696.

Traka, M.H. (2016) Chapter Nine—health benefits of glucosinolates. In: Kopriva, S. (Ed.) Advances in botanical research *glucosinolates*. Cambridge, Massachusetts: Academic Press, pp. 247–279.

Tran, H., Ficke, A., Asiimwe, T., Höfte, M. & Raaijmakers, J.M. (2007) Role of the cyclic lipopeptide massetolide A in biological control of *Phytophthora infestans* and in colonization of tomato plants by *Pseudomonas fluorescens*. *New Phytologist*, 175, 731–742.

Van der Ent, S., Van Wees, S.C.M. & Pieterse, C.M.J. (2009) Jasmonate signaling in plant interactions with resistance-inducing beneficial microbes. *Phytochemistry*, 70, 1581–1588.

Walker, V., Bertrand, C., Bellvert, F., Moënne-Loccoz, Y., Bally, R. & Comte, G. (2011) Host plant secondary metabolite profiling shows a complex, strain-dependent response of maize to plant growth-promoting rhizobacteria of the genus Azospirillum. *New Phytologist*, 189, 494–506.

Weston, D.J., Pelletier, D.A., Morrell-Falvey, J.L., Tschaplinski, T.J., Jawdy, S.S., Lu, T.-Y. et al. (2012) *Pseudomonas fluorescens* Induces Strain-Dependent and Strain-Independent Host Plant Responses in Defense Networks, Primary Metabolism, Photosynthesis, and Fitness. *Molecular Plant-Microbe Interactions®*, 25, 765–778.

Xiao, J., Capanoglu, E., Jassbi, A.R. & Miron, A. (2016) Advance on the flavonoid c-glycosides and health benefits. *Critical Reviews in Food Science and Nutrition*, 56, S29–S45.

Xie, D.-Y., Sharma, S.B., Paiva, N.L., Ferreira, D. & Dixon, R.A. (2003) Role of anthocyanidin reductase, encoded by BANYULS in plant flavonoid biosynthesis. *Science*, 299, 396–399.

Xuan, L., Zhang, C., Yan, T., Wu, D., Hussain, N., Li, Z. et al. (2018) TRANSPARENT TESTA 4-mediated flavonoids negatively affect embryonic fatty acid biosynthesis in Arabidopsis. *Plant, Cell & Environment*, 41, 2773–2790.

Yin, R., Han, K., Heller, W., Albert, A., Dobrev, P.I., Zažímalová, E. et al. (2014) Kaempferol 3-O-rhamnoside-7-O-rhamnoside is an endogenous flavonol inhibitor of polar auxin transport in Arabidopsis shoots. *New Phytologist*, 201, 466–475.

Yonekura-Sakakibara, K., Tohge, T., Matsuda, F., Nakabayashi, R., Takayama, H., Niida, R. et al. (2008) Comprehensive flavonol profiling and transcriptome coexpression analysis leading to decoding gene–metabolite correlations in Arabidopsis. *The Plant Cell*, 20, 2160–2176.

SUPPORTING INFORMATION

Additional supporting information can be found online in the Supporting Information section at the end of this article.

How to cite this article: Jeon, J.-S., Rybka, D., Carreno-Quintero, N., De Vos, R., Raaijmakers, J.M. & Etalo, D.W. (2022) Metabolic signatures of rhizobacteria-induced plant growth promotion. *Plant, Cell & Environment*, 1–14. https://doi.org/10.1111/pce.14385